Wasit Journal of Engineering Sciences

Journal homepage: https://ejuow.uowasit.edu.iq

Modeling and Simulation of the Erosion Rate in Hydraulic Structures

Shams M. Cheyad [1], Ali N. Hilo [1], Thaar S. Al-Ghasham [1], Ali Hameed Abd [2], and Rawaa H. Ismaeil [1].

Affiliations
1 Civil Engineering Department, University of Wasit, Iraq

2 Mechanical Engineering Department, University of Wasit, Iraq.

Correspondence
Shams M. Cheyad
Department of Civil Engineering, University of Wasit, Wasit, Iraq
Email: shamsalnahar9582@gmail.com

Received
28-October-2021
Revised
08-December-2021
Accepted
10-January-2022
Doi: 10.31185/ejuow.Vol10.Iss1.239

Abstract

Basically, the durability of hydraulic structures is heavily influenced by concrete surface resistance against mechanical wear. Hydro-abrasion is the term used to describe deterioration of concrete surface inflicted by the continuous removal of surface material due to the effect of water-dragged solids. This type of cumulative damage for the surface of concrete may be seen in practically all hydraulic systems, in varying degrees of severity. Essentially, such hydro-abrasive concrete wear reduces the life time of the hydraulic structure, and as a result of the maintenance necessary, the facility's non-operation during the repair time increases costs. The numerical simulation was carried out according to the Messa device. Then, after an excellent agreement had been achieved with the experiments, a parametric study was implemented, where three key factors were investigated: the flow inclination angle, the density (sand concentration in water) and the rotational speed of the water. ANSYS 19.0 was used for simulating the erosion rate. According to the directed numerical simulation, the best flow inclination angle was at 45º, which showed lowest erosion rate. In addition, the findings showed that, the erosion rate raised considerably as the density and rotational speed increased.

Keywords: concrete erosion, hydraulic structures, ANSYS

الخلاصة: تعتمد متانة الهياكل الهيدروليكية بشكل أساسي على مقاومة سطح الخرسانة للتآكل الميكانيكي. الكشط المائي هو المصطلح المستخدم لوصف الضرر السطحي الناتج عن الإزالة المستمرة للمواد الناتجة عن تأثير الجسيمات الصلبة المنقولة بالماء. يمكن ملاحظة هذا النوع من التدهور التدريجي للأسطح الخرسانية في جميع المنشآت الهيدروليكية تقريبًا ، بدرجات متفاوتة من الشدة. بشكل أساسي ، يؤدي تآكل الخرسانة هذا إلى تقليل العمر الافتراضي للمنشآت المائية ، ونتيجة للإصلاحات اللازمة ، يؤدي عدم تشغيل المنشآت أثناء وقت الإصلاح إلى زيادة التكاليف. تم إجراء المحاكاة العددية باستخدام وفقاً لجهاز **(Messa)** ، وبعد التوصل إلى اتفاق ممتازمع نتائج التجارب ، تم تنفيذ دراسة بارامترية ، حيث تم فحص ثلاثة عوامل رئيسية: زاوية ميل التدفق ، والكثافة (تركيز الرمال في الماء) وسرعة دوران الماء. تم استخدام **ANSYS 19.0** لمحاكاة معدل التآكل. وفقًا للمحاكاة العددية ، كانت أفضل زاوية ميل للجريان عند ٤٥ درجة ، والتي أظهرت أقل معدل تآكل. بالإضافة إلى ذلك ، أظهرت النتائج أن معدل التآكل يزداد مع زيادة الكثافة والسرعة الدورانية.

1. INTRODUCTION

Hydraulic structures are typically made of concrete. As a result, abrasion-induced erosion has been identified as one of the most significant issues encountered during their work. Decomposition occurs as a result of the loads caused by the water flow of the transported sediment. When high water flow velocities are faced, this becomes a serious problem [1,2]. This type of deterioration occurs in three steps. First and foremost, pre-abrasion scrubbing occurs, water velocity and pressure are the governing parameters at this step. Second, waterborne particles impinge on the concrete surface, causing it to crack. The abrasion rate is affected by the properties of the carried materials, such as their form, hardness, size, and density. Furthermore, the rate of abrasion damage is highly dependent on the velocity of the flowing water. Water at a higher velocity can easily move sediments of greater

size and quantity, resulting in heavier abrasion [3,4]. To assess the abrasive wear that happens in hydraulic structures, a variety of standard and non-standard test methodologies are used. The underwater approach is the most typical test. Steel balls of various sizes are used to simulate water-borne particles [1]. Messa et al. [6], proposed a new test procedure. When the steel balls are replaced with a defined silica sand quantity, it can be regarded as a modification to the underwater approach in order to offer an actual simulation of the abrasive impact of waterborne solids in hydraulic structures.

According to numerous experts, abrasion rate is influenced by a variety of elements, including, the fibers inclusion and cementitious materials addition, compressive and tensile strength, age of concrete, and the angle of impact between flowing water and concrete surface [4,5]. These variables can be divided into two groups: first, that is directly related to the properties of concrete, and second, that are dependent on the environment surrounding hydraulic structures, such as abrasive particle characteristics and fluid flow angle [7]. The abrasion resistance of concrete was found to increase as the concrete strength or the water-to-cement ratio was reduced, based on the characteristics of the concrete [3,8]. The abrasion resistance was observed to be improving when fibers were added to the concrete mixture [9]. Another study found that when the amount of cement was substituted with silica fume, abrasion erosion was reduced [10].

In this work, the ANSYS Fluent 19.0 was used to conduct a CFD simulation as a numerical study to investigate how the abrasion rate influenced the concrete samples at various impact angles, densities, and velocities of the abrasive particles. the Discrete Phase Method (DPM) was used to solve the flow of water and abrasive sand particles.

2. NUMERICAL PROCEDURE

ANSYS Fluent was chosen as a primary simulation tool for the study in order to investigate the surface erosion damage of the concrete sample. The research is based on the modeling of abrasion erosion on a concrete surface using a 45º paddle angle, density (sand particles concentration in water) was 28 kg/m3, and rotational speed was 600 rpm according to Messa device. The CFD simulation was validated first with the experimental findings. Then, after an excellent agreement had been achieved, a parametric study was implemented, where three key factors were investigated: paddle angles of (30º and 60º), the density of (35 and 45 kg/m3), and the rotational speeds of (900 and 1200 rpm).

The transient-state simulation of the concrete specimen model was used, and the fluid was assumed to be incompressible; in addition, the K-epsilon model was used for the viscous model.

3. NUMERICAL MODELING

3.1.Governing equations

The governing equations on which the ANSYS program is based include the continuity equation and momentum equation. Moreover, depending on the nature of the flow, equations such as the energy equation and the turbulence equation may be required to properly and satisfactorily solve the flow problems [1].

-The continuity equation

$$(\delta \mathrm{Vx}/\delta x) + (\delta Vy/\delta y) + (\delta Vz/\delta z) = 0 \quad (1)$$

whereVx, Vy, and Vz are velocity components in directions x, y, and z.

- Momentum equation

1. Momentum Equation in the X-direction

$$v_x \frac{\partial v_x}{\partial_x} + v_y \frac{\partial v_x}{\partial y} + v_z \frac{\partial v_x}{\partial z} = -\frac{1}{\rho}\frac{\partial P}{\partial x} + \upsilon\left(\frac{\nabla^2 v_{\eta x}}{\partial x^2} + \frac{\nabla^2 v_x}{\partial y^2} + \frac{\nabla^2 v_x}{\partial z^2}\right) \quad (2)$$

2. Momentum Equation in the Y-direction

$$v_x\frac{\partial v_y}{\partial_x}+v_y\frac{\partial v_y}{\partial y}+v_z\frac{\partial v_y}{\partial z}=-g-\frac{1}{\rho}\frac{\partial P}{\partial x}+\upsilon\left(\frac{\nabla^2 v_y}{\partial x^2}+\frac{\nabla^2 v_y}{\partial y^2}+\frac{\nabla^2 v_y}{\partial z^2}\right) \quad (3)$$

3. Momentum Equation in the z-direction

$$v_x\frac{\partial v_z}{\partial_x}+v_y\frac{\partial v_z}{\partial y}+v_z\frac{\partial v_z}{\partial z}=-\frac{1}{\rho}\frac{\partial P}{\partial x}+\upsilon\left(\frac{\nabla^2 v_z}{\partial x^2}+\frac{\nabla^2 v_z}{\partial y^2}+\frac{\nabla^2 v_z}{\partial z^2}\right) \quad (4)$$

where, u = [V_x, V_y, V_z], g are velocity vector, *P* represents the pressure of the fluid, ρ refers to the density of the fluid,∇^2 represents the Laplacian operator and ∂v represents the gradient of velocity.

3.2.Geometry formation

The 3-D geometry is sketched by ANSYS Fluent 19.0 for the tank and the impeller zone with different paddle angles of (30º, 45º and, 60º). Three forms of geometries were used in this study that depends on the angle of the paddle as shown in Figure 1.

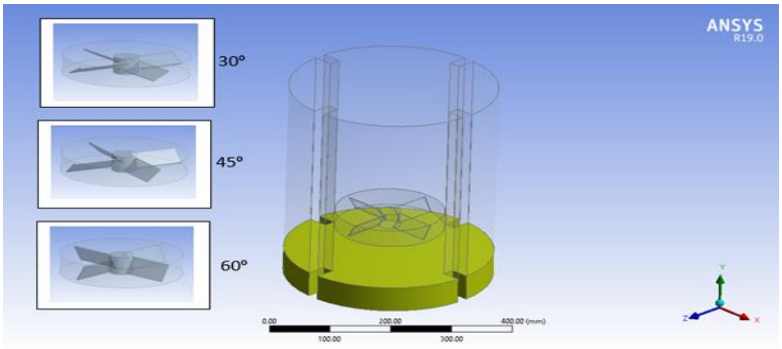

Figure 1 Geometry of the model.

3.3.Mesh creation

The three models generated, as shown in Figure 2, are meshed using a tetrahedron mesh with the number of nodes and elements uncovered in Table 1.

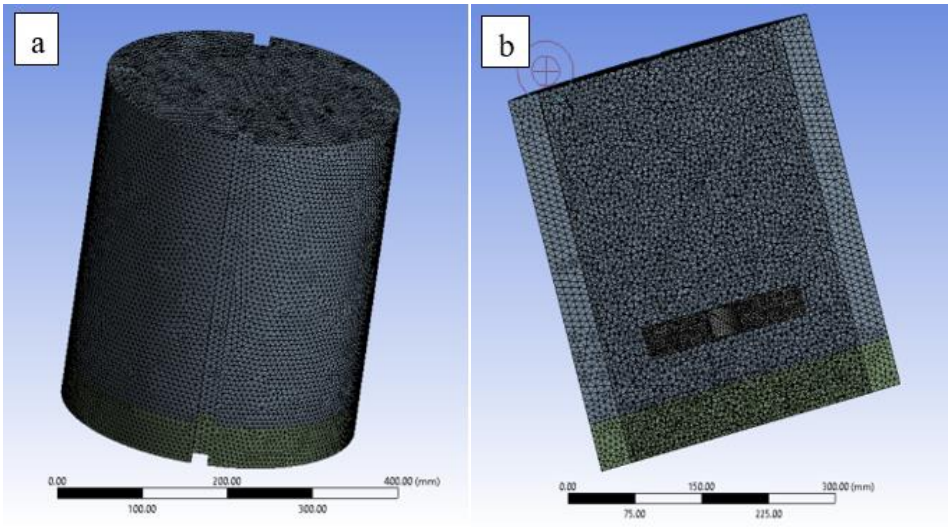

Figure 2 (a) Model mesh; (b) Section plane in Mesh model.

Table 1 Elements and nodes number.

No.	Geometry	Number of Elements	Number of Nodes
1	Angle 30º	1105916	197834
2	Angle 45º	1106025	197834
3	Angle 60º	1105335	197677

4. DISCRETE PHASE METHOD

In FLUENT, the DPM was applied for simulating the movements and interactions of the fluid and solid particles. As momentum between particles and fluid occurs, FLUENT provides the option to include or remove these impacts by using the Uncoupled or Coupled discrete phase method. If there is no impact for particles on the solution of flow, the uncoupled DPM must be used, while if there is an impact, the coupled DPM provides the best choice.

The condition of local continuous phase can be applied for solving the equation of particle force balance, as the following formula [11].

$$\frac{du_p}{dt} = F_D(u - u_p) + \frac{g_x(\rho_p - \rho)}{\rho_p} + F_x \tag{5}$$

where, $u_p$and u represent the particle and fluid velocity, respectively, ρ_p and ρ represent the density of particle and fluid, respectively, g represents the gravitational acceleration, F_x can be used for accounting additional forces, $F_D(u - u_p)$ represents the force of drag per particle mass unit.

5. EROSION MODEL

The model of erosion is included in ANSYS software [12]. The rate of erosion can be determined by ANSYS, mass flow products, and functions of the particle diameter, angle of impact, and speed due to the given formula [13].

$$R_{erosion} = \sum_{p=1}^{N} \frac{m_p C(d_p) f(\alpha) v^{b(v)}}{A_{fice}} \tag{6}$$

where C(d_p) represents a particle function, $f(\alpha)$ represents a function of impact angle, α represents the impact angle of the particle path with the face of a wall, v represents the particle's relative velocity, b(v) represents a function of the particle's relative velocity, and A_{fice} refers to the area of the cell face at the wall.

6. BOUNDARY CONDITIONS

1. The rotational speeds were 600, 900 and, 1200 rpm.
2. The sand particle diameter is 1.5 mm with a density of 2650 kg/m3.
3. Three paddle angles were used (30º,45º and, 60º).
4. Three different densities (sand concentration in water) were used (28, 35 and, 45 kg/m3).
5. density is 2300 kg/m3 for concrete samples.
6. The atmospheric pressure is the pressure outlet.

7. RESULTS AND DISCUSSION

7.1.Effect of paddle angles on erosion rate

The influence of the paddle angle was investigated numerically with a density of 28 kg/m3 and rotational speed of 600 rpm. As shown in Figure 3, the maximum erosion rate is noticeable when the paddle angle is 60°, while it was the lowest value for the 45° angle. The inclination flow angle was efficient on the cross-sectional surface of the

specimen when the angle was 60º, causing severe abrasion and increasing the rate of erosion. The trend of curves in Figure 4 showed that when the paddle angle was 30º, the erosion rate rose dramatically. Then when the angle was altered to 45º, the erosion rate began to decline by about 25%. After that, when the paddle angle was set to 60º, the erosion rate returned to develop by about 36.5%.

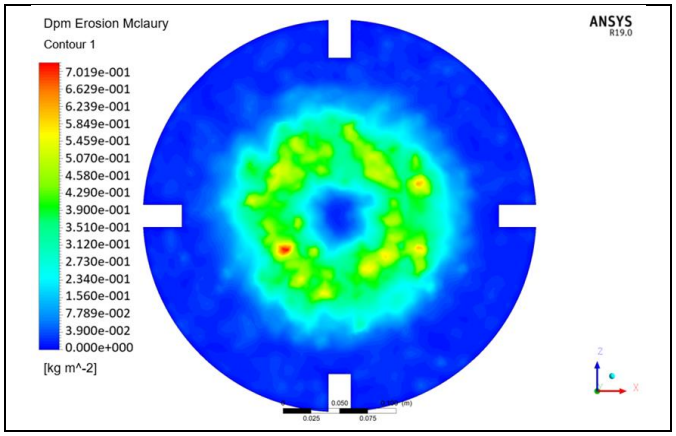

(a)

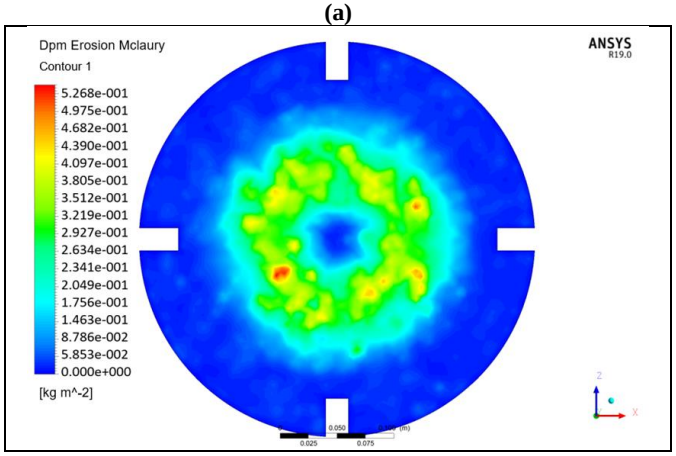

(b)

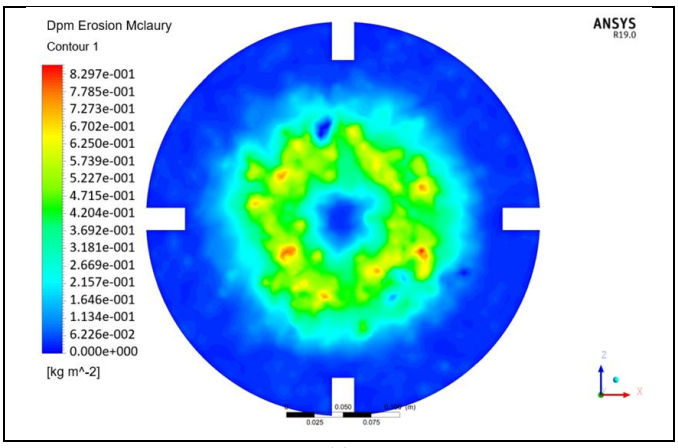

(c)

Figure 3 Erosion rates using various impact angles of; (a) 30º ;(b) 45º; and (c) 60º.

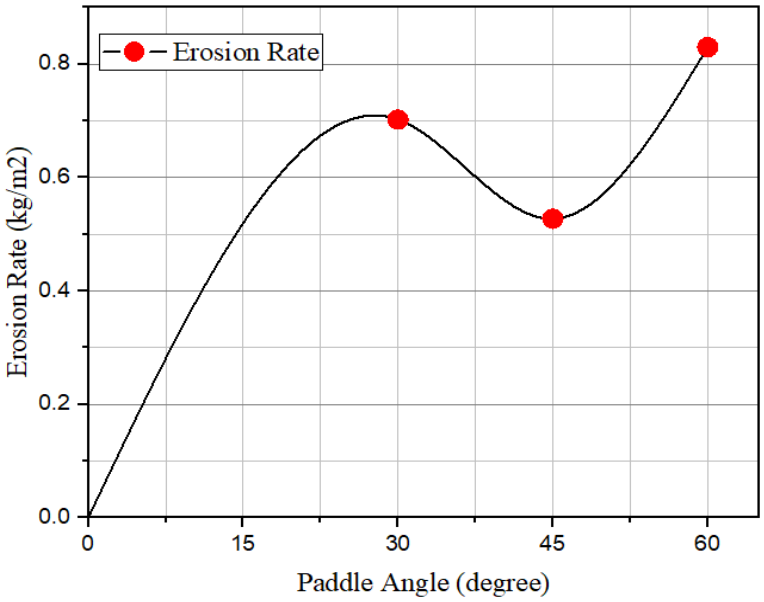

Figure 4 Erosion Rate with different paddle angles

7.2.Effect of the density (sand concentration in winter) on the erosion rate

This study was applied to the angle of 60º, which is considered the worst-case; as previously mentioned, it suffers from the most considerable erosion rate, so this case was studied numerically with different densities of (35, and 45 kg/m3) with a rotational speed of 600 rpm. When the concentration of sand in water increases, it means an increase in the number of sand particles that hit the surface of the concrete, which causes an increase in the rate of erosion. Figure 5 presents the effects of the various densities on the erosion rate at the sample surfaces. The maximum value of erosion for 28, 35, and 45 kg/m3 where 8.279e-001, 9.285e-001 and 1.119e+000 kg/m2 respectively. Therefore, the relationship between the erosion rate and density is a direct correlation; when the density increases, the erosion rate increases, the erosion rate for 35 and 45 kg/m3 increased by about 10.8 and 25.8%, respectively, as shown in Figure 6.

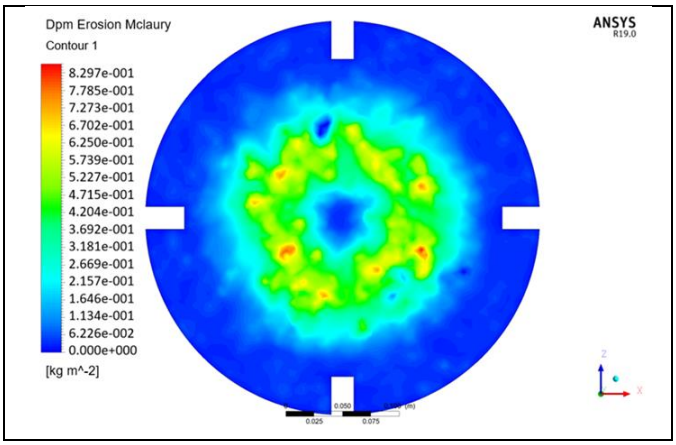

(a)

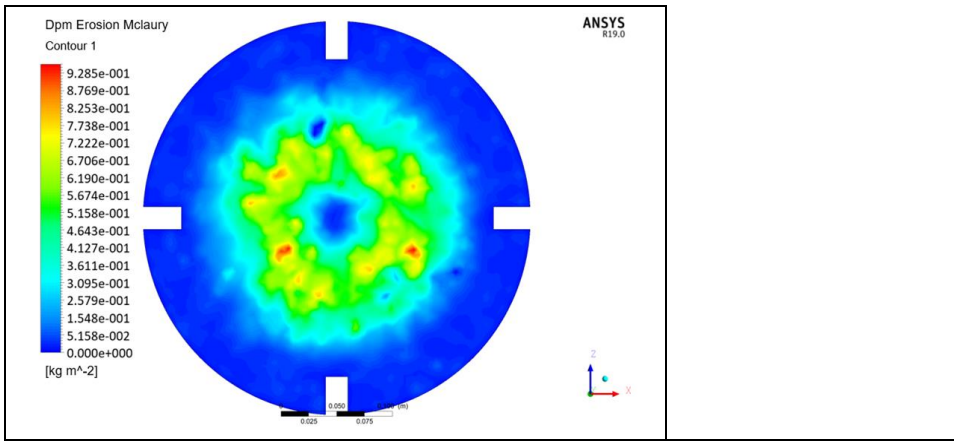

(b)

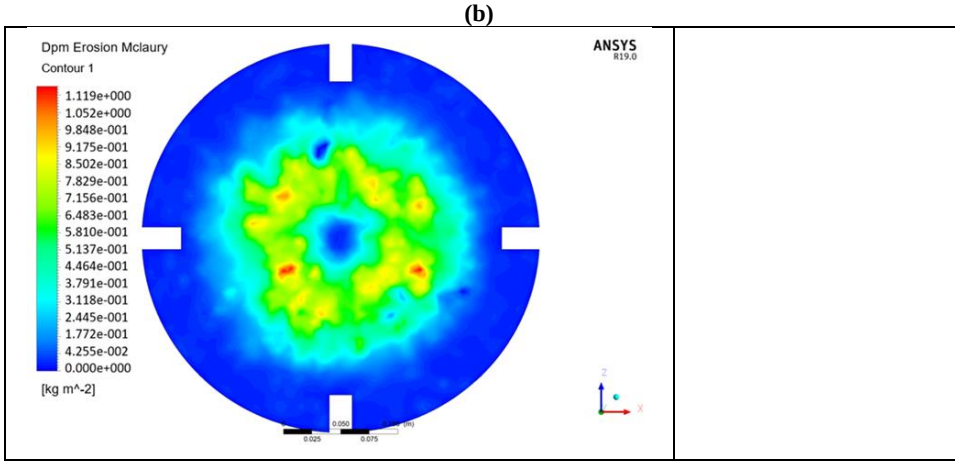

(c)

Figure 5 DPM Erosion Rate with density (a) 28 kg/m3, (b) 35 kg/m3, and (c) 45 kg/m3

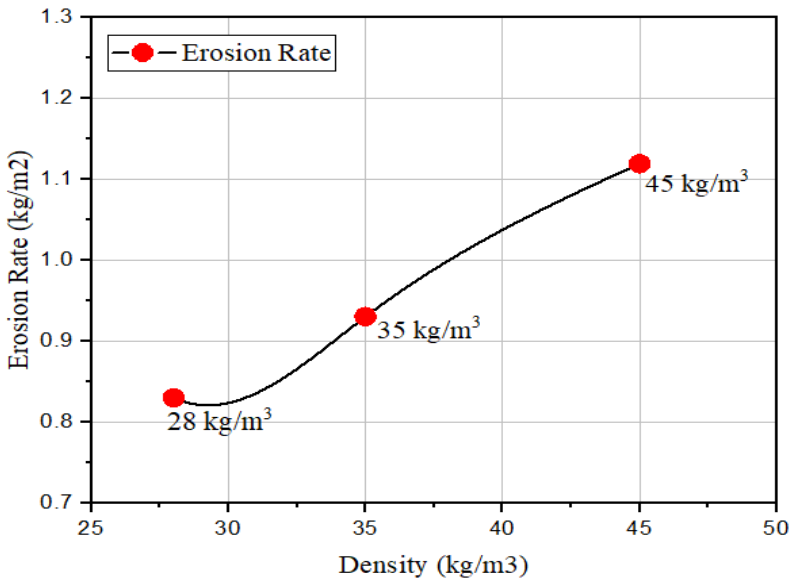

Figure 6 Erosion rate with different densities

7.3.Influence of paddle speed on the rate of erosion

The effect of paddle speed on the erosion rate was studied at an angle of 60º and density of 28 kg/m3 with different speeds of 600, 900, and 1200 rpm. When the paddle speed increases, the speed of collision of sand particles with the concrete surface increases, which leads to a rise erosion rate. Figure 7 shows the relationship between the paddle speed and the erosion rate, from the Figure it is clear that the increased rotational speed increases the erosion rate. The erosion rate increment due to the raise of paddle speed of 900 and 1200 rpm were about 58.7% and 73.3%, respectively. Figure 8 shows the erosion rate with different paddle speeds.

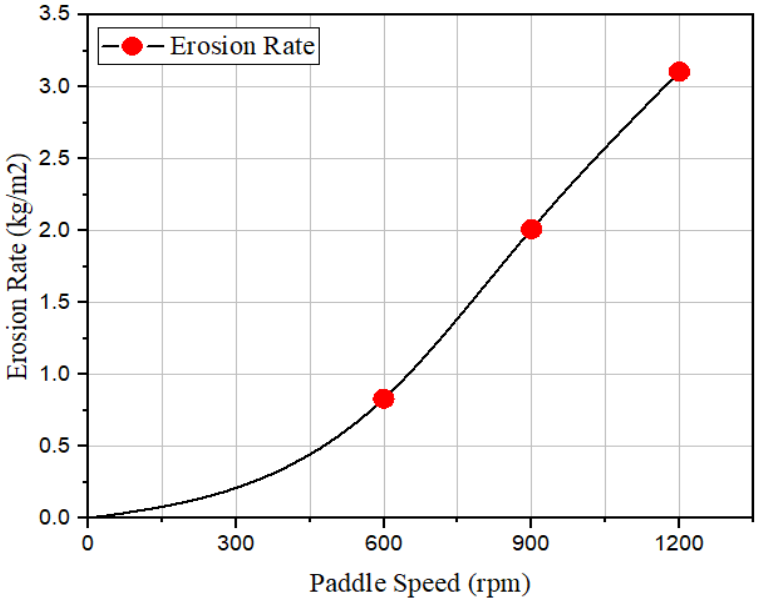

Figure 7 Erosion Rate with a different paddle speed

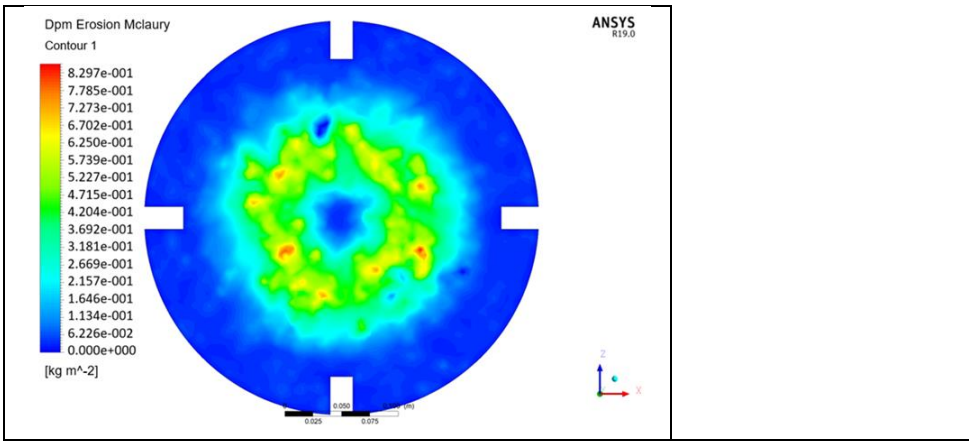

(a)

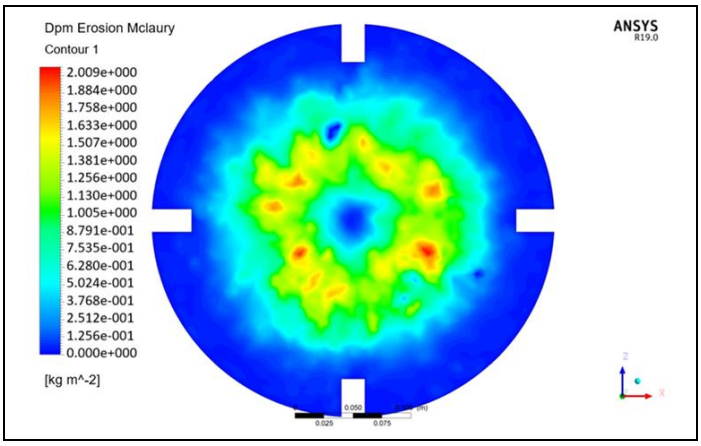

(b)

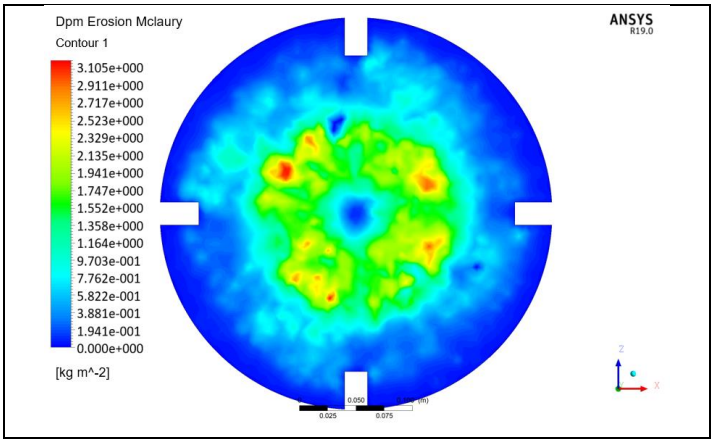

(c)

Figure 8 Erosion Rate at (a) 600 rpm; (b) 900 rpm ,and (c) 1200 rpm

8. CONCLUSION

1. DPM was utilized in this study to measure and forecast the produced erosion by water-borne particles. Several aspects have been considered, including the angle of impact, density, particle size, the flowing water velocity, and the overall rate of flow of the discrete phase model.
2. According to the results of this simulation, an impact angle of 60º has the highest rate of erosion. While the erosion rate is reduced when the inclination flow angle is 45º.
3. The density (sand concentration in water) has a significant effect on the erosion rate. It has been observed that the erosion rate increases as the density increases. For example, the erosion rate increased about 10.8 and 25.8% for densities of 35 and 45 kg/m3, respectively.
4. The erosion damage increases when the rotational speed increases, as the erosion rate improved by about 58.7 and 73.3% when the rotational speed was 900 and 1200 rpm, respectively
5. For all three impact angles (30º, 45º, and 60º), CFD simulations are capable of forecasting and obtaining a fully developed profile of velocity, pressure, and well shear on the concrete surface.

REFERENCES

1. Hilo, A. N., Ghasham, T. S., Hamedi, M. H., Ayoob, N. S., & Abd, A. H. (2019, October). Numerical and experimental study of abrasion erosion in hydraulic structures

of high-velocity water flow. *In 2019 12th International Conference on Developments in eSystems Engineering (DeSE)*: 415-420. IEEE.

2. Ismaeil, R. H., Hilo, A. N., Al-Gasham, T. S., & Abd, A. H. (2021). Concrete Erosion Modelling by Water Jet using Discrete Phase Method. *In IOP Conference Series: Materials Science and Engineering* **1058** (1), p. 012032). IOP Publishing.
3. Abid, S. R., Hilo, A. N., Ayoob, N. S., & Daek, Y. H. (2019). Underwater abrasion of steel fiber-reinforced self-compacting concrete. *Case Studies in Construction Materials*, **11**, e00299.
4. Abid, S. R., Hilo, A. N., & Daek, Y. H. (2018). Experimental tests on the underwater abrasion of engineered cementitious composites. *Construction and building materials*, **171**: 779-792.
5. Turk, K., & Karatas, M. (2011). Abrasion resistance and mechanical properties of self-compacting concrete with different dosages of fly ash/silica fume.
6. Messa, G. V., Branco, R. D. L., Dalfre Filho, J. G., & Malavasi, S. (2018). A combined CFD-experimental method for abrasive erosion testing of concrete.
7. Abid, S. R., Shamkhi, M. S., Mahdi, N. S., & Daek, Y. H. (2018). Hydro-abrasive resistance of engineered cementitious composites with PP and PVA fibers. *Construction and Building Materials*, **187**:168-177.
8. Shamsai, A., Peroti, S., Rahmani, K., & Rahemi, L. (2012). Effect of water-cement ratio on abrasive strength, porosity and permeability of nano-silica concrete. *World Applied Sciences Journal*, **17**(8), 929-933.
9. Grdic, Z. J., Curcic, G. A. T., Ristic, N. S., & Despotovic, I. M. (2012). Abrasion resistance of concrete micro-reinforced with polypropylene fibers. *Construction and Building Materials*, **27**(1): 305-312.
10. Liu, Y. W. (2007). Improving the abrasion resistance of hydraulic-concrete containing surface crack by adding silica fume. *Construction and Building Materials*, **21**(5): 972-977.
11. Momber, A. W. (2016). A probabilistic model for the erosion of cement-based composites due to very high-speed hydro-abrasive flow. *Wear*, **368**: 39-44.
12. Ansys, I. (2013). Fluent theory guide. ANSYS Inc, USA [(accessed on 27 March 2020)].
13. Fluent, A. N. S. Y. S. (2013). ANSYS Fluent User's Guide r15. Chapter, 6, 223-247.